

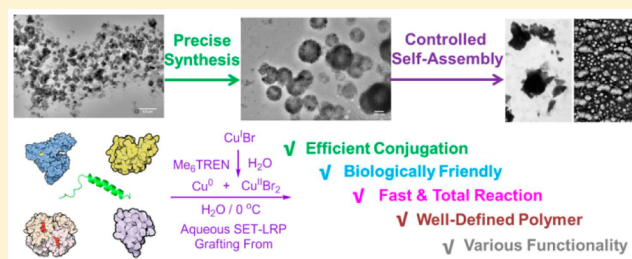
# Well-Defined Protein/Peptide–Polymer Conjugates by Aqueous Cu-LRP: Synthesis and Controlled Self-Assembly

Qiang Zhang, Muxiu Li, Chongyu Zhu, Gabit Nurumbetov, Zaidong Li, Paul Wilson, Kristian Kempe, and David M. Haddleton\*

Department of Chemistry, University of Warwick, CV4 7AL, Coventry, United Kingdom

**S** Supporting Information

**ABSTRACT:** The synthesis of well-defined protein/peptide–polymer conjugates with interesting self-assembly behavior via single electron transfer living radical polymerization in water is described. A range of protein/peptides with different physical and chemical properties have been modified to macroinitiators and optimized polymerization conditions ensure successful polymerization from soluble, insoluble, and dispersed protein/peptide molecules or protein aggregates. This powerful strategy tolerates a range of functional monomers and mediates efficient homo or block copolymerization to generate hydrophilic polymers with controlled molecular weight (MW) and narrow MW distribution. The polymerizations from bovine insulin macroinitiators follow surface-initiated “grafting from” polymerization mechanism and may involve a series of self-assembly and disassembly processes. Synthesized insulin-polymer conjugates form spheres in water, and the self-assembly behavior could be controlled via thermal control, carbohydrate–protein interaction, and protein denaturation.



## 1. INTRODUCTION

Bioconjugation of functional polymers to therapeutic proteins and peptides can endow improved biopharmaceutical properties through multiple mechanisms including size enlargement, charge modification, protein repellence, and epitope shielding, etc.<sup>1,2</sup> PEGylation is regarded as one of the most successful bioconjugation techniques in which biocompatible poly(ethylene glycol) (PEG) is covalently attached to therapeutic proteins and peptides. Most protein–polymer drugs approved for present clinical use are produced by PEGylation of native proteins in order to obtain improved pharmacokinetics, prolonged blood circulation, and decreased immunogenicity while maintaining an acceptable level of biological activity.<sup>3–5</sup> However, PEG has drawbacks including tissue uptake and accumulation, causing potential hypersensitivity and non-biodegradability, which encourage the development of new biocompatible polymers as potential PEG alternatives.<sup>3,6,7</sup>

The target of bioconjugation is site-specific modification of proteins and peptides with well-defined polymers without reducing the biomolecule activity below an acceptable level. Compared with the direct reaction of terminal functional polymers with protein/peptides which can suffer from low conjugation efficiency often requiring extensive postreaction purification, *in situ* grafting of polymers from protein/peptides, “grafting from” conjugation methodology, shows some promise in addressing these issues. This methodology has emerged as powerful and popular technology for bioconjugation in the past decade mostly due to the development of living radical polymerization (LRP). It is generally performed through synthesis of protein/peptide derived macroinitiators, or macro

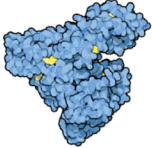

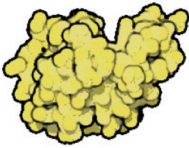


chain transfer agents (CTAs), via transformation with small molecule initiators or CTA’s prior to polymerization from these conjugation sites. This can significantly improve conjugation efficiency due to minimizing steric effects and allowing for relatively facile purification while maintaining controlled MW and narrow MW distribution of the final polymers.<sup>8</sup> At the same time, it places demands on the polymerization conditions such as choice of solvent, temperature, concentration, and catalyst, which needs to be friendly to the often fragile protein/peptides and also be sufficiently efficient to mediate polymerization at low concentration and temperature. In many cases the polymerization is required to be performed in aqueous media due to solubility constraints and at relatively low temperature in order to preserve biological activity.

Copper-mediated living radical polymerization (Cu-LRP), in particular, atom-transfer radical polymerization (ATRP), was the first successful LRP method used for *in situ* polymer conjugation from protein/peptides.<sup>9–13</sup> Indeed Cu<sup>I</sup>X/N-ligand complexes have been used as the catalyst in aqueous media, however, the products generally have relatively broad MW distribution ( $M_w/M_n > 1.3$ ).<sup>10</sup> Thus, it has generally been regarded as a challenge to perform ATRP in water to well-defined hydrophilic polymers with narrow MW distribution due to the extremely high activation rate and inefficient deactivation as well as several side reactions related to deactivator stability, catalyst disproportionation, and polymer terminal group loss.<sup>14,15</sup> Only ligands that form very stable Cu<sup>I</sup> complexes

Received: April 21, 2015

Published: July 7, 2015

Table 1. Schematic Representation of the Proteins Used in This Research and Their Relative Typical Properties

Name	Bovine serum albumin (BSA)	Bovine haemoglobin (Hb)	Human lysozyme (Lysozyme)	Salmon calcitonin (sCT)	Bovine insulin (Insulin)
Structure					
Average mass (Da)	69293 <sup>a</sup>	~ 65000 <sup>a</sup>	16537 <sup>a</sup>	3432	5733
Isoelectric point (pI)	4.9	6.8	9.4 <sup>a</sup>	8.9 <sup>a</sup>	5.3
Initiator number	~ 29 <sup>b</sup>	~ 12 <sup>b</sup>	~ 5 <sup>b</sup>	~ 2 <sup>b</sup>	1 ~ 3 <sup>b</sup>
Property	Typical water-soluble protein with high MW	Protein bears iron & porphyrin ring and binds copper cation	Modified protein with poor water-solubility	Simple low MW polypeptide	Modified peptide self-assemblies in water

<sup>a</sup>The data was cited from Uniport and the pI value was computed by ExPASy. Other MW and pI data was from supplier. <sup>b</sup>The average initiator number per protein/peptide was calculated according to relative MW increase on MADL-ToF MS spectrum as shown in SI.

are usually recommended for ATRP in aqueous media, while ligands with high activity including tris(dimethylamino)ethyl amine (Me<sub>6</sub>TREN) and *N,N,N',N',N''*-pentamethyl diethylenetriamine (PMDETA) have not been used due to fast rates and extent of disproportionation of Cu<sup>I</sup>.<sup>14,16</sup> ATRP with different initiation processes has been established for use in water, such as activators generated by electron transfer (AGET) ATRP, etc., which maintain a low ratio of [Cu<sup>I</sup>]/[Cu<sup>II</sup>] via the slow addition of a reducing agent inducing improved control over MW distribution when grafting from proteins.<sup>17–19</sup>

Single electron-transfer living radical polymerization (SET-LRP) has drawn attention due to the ability to mediate fast polymerization of both activated and nonactivated vinyl monomers, generating well-defined polymers with complex structure, various functionality, high MW, and high chain end fidelity capable for full conversion multiblock copolymerization.<sup>20–26</sup> SET-LRP requires an appreciable disproportionation of Cu<sup>I</sup> in polar solvents to active Cu<sup>0</sup> and Cu<sup>II</sup>. Thus, conditions such as high solvent polarity and unstable Cu<sup>I</sup> complexes are required for efficient SET-LRP. Disproportionation of Cu<sup>I</sup> to Cu<sup>0</sup> and Cu<sup>II</sup> in water is thermodynamically driven via very high heats of formation of Cu<sup>II</sup> aqua salts, going fast, quantitatively and irreversibly, unless the Cu<sup>I</sup> is stabilized by  $\pi$ -acceptor ligands.<sup>22,27–30</sup> Thus, water is an excellent solvent for SET-LRP, and indeed progress on polymerization of hydrophilic monomers in water has been achieved by SET-LRP in recent years.<sup>20,29,31–38</sup> Fast SET-LRP of various monomers has been shown to give well-defined polymers at ambient and subambient temperatures with full conversion obtained in minutes. The chemistry shows a remarkable tolerance toward complex solvents, including beers, wines, and blood serum,<sup>50–52</sup> and the high chain end fidelity allows for the construction of multiblock copolymers as well as the ability of unrestricted switches between acrylates and acrylamides during copolymerization, which all demonstrate the potential of SET-LRP for the synthesis of biofunctional polymers.<sup>31,39–41</sup> As such, SET-LRP can be regarded at least as an equivalent technique to reversible addition–fragmentation chain transfer (RAFT) polymerization, which has been shown to be a suitable bioconjugation technique due to its advantageous properties.<sup>42–44</sup> Protein macro CTAs have been prepared and used for RAFT polymerization via initiation through  $\gamma$  ray<sup>23</sup> and visible

light<sup>45–47</sup> irradiation or by reaction with ambient temperature azo-initiators.<sup>48,49</sup>

Cu<sup>0</sup> in the form of wire or powder, either from commercial sources or *in situ* generated by disproportionation of Cu<sup>I</sup>, works as an activator allowing for polymerization initiation from protein/peptide macroinitiators. Moreover, the Cu<sup>0</sup> activator should be less susceptible to interference from protein/peptides, which contain polar groups, such as amines and acids, etc., that can effectively complex with copper cations.<sup>50,51</sup>

Limited research has been carried out on the synthesis of protein/peptide–polymer conjugates by SET-LRP, and this directed our research toward the modification of a small range of protein/peptides with different polymers, including biocompatible poly(PEG), environmentally responsive poly(*N*-isopropylacrylamide, NIPAM), and biofunctional glycopolymers. We aimed to develop a versatile Cu-LRP strategy for *in situ* polymer modification of protein/peptides bearing different properties under biofriendly conditions. Polymerization parameters including reaction conditions (catalyst, solvent, and temperature, etc.) and postpolymerization processes as well as properties of obtained conjugates and relative polymers were studied and discussed.

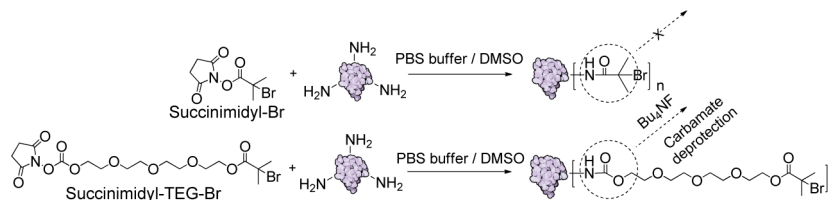
In addition protein/peptide–polymer conjugates have shown interesting self-assembly behavior due to protein interactions, peptide chain folding, and multiblock copolymer structures, which favor the formation of various nanostructures and gels with different applications.<sup>52–60</sup> In our research bovine insulin formed different nanostructures during the macroinitiator synthesis and aqueous polymerization. The morphologies of assemblies could also be controlled utilizing different strategies, and our preliminary results are reported.

## 2. RESULTS AND DISCUSSION

### 2.1. Synthesis and Characterization of Protein/Peptide Macroinitiators.

Rather than site-specific modification, our focus was the synthesis of a series of protein/peptide macroinitiators with varied properties, which will represent as models for polymerization under different conditions. The major considerations were: MW, water-solubility, and the presence of different functional groups. Activated *N*-hydroxysuccinimide (NHS) esters have been commonly employed as amine-reactive groups in bioconjugation chemistry. This one-step aminolysis reaction almost suits any amine-containing

Scheme 1. Schematic Representation for the Synthesis of Protein/Peptide Macroinitiators via NHS Chemistry



protein/peptides and allows for the facile synthesis of protein macroinitiators or protein–polymer conjugates and thus suits our demand.<sup>12,18</sup> In this current work five commercially available proteins and peptides were employed, including bovine serum albumin (BSA), bovine hemoglobin (Hb), human lysozyme (lysozyme), salmon calcitonin (sCT), and bovine insulin (insulin) (Table 1). All of the proteins and peptides possessed primary amine groups at the N-terminus of each peptide chain and side-chain lysine amino acid residues, which were utilized to react with NHS-ester activated initiators under slightly alkaline conditions (pH = 8.0) (Scheme 1).

The reaction with succinimidyl-tetraethylene glycol-Br (succinimidyl-TEG-Br) yielded ester-based macroinitiators with a carbamate tetraethylene glycol linker, which is susceptible to mild cleavage with  $\text{Bu}_4\text{NF}$  thus enabling further characterization of the “grafted from” polymer chains.<sup>18,61</sup> Stable amide-based macroinitiators were prepared via reaction with succinimidyl-Br as control experiments.

BSA is water-soluble and contains different functional amino acids such as lysine and cysteine, which can be targeted for modification. The reaction with succinimidyl-TEG-Br was efficient as demonstrated by matrix-assisted laser desorption ionization time-of-flight mass spectrometry (MALDI-ToF MS) (Figure S3), which indicated that every BSA-TEG-Br contains ~29 bromine atoms on average. Sodium dodecyl sulfate-polyacrylamide gel electrophoresis (SDS PAGE) of BSA-TEG-Br showed a slight MW increase compared with native BSA, and it also revealed presence of impurities in the commercial product (Figure S4).

Hb was chosen as it is an iron-containing metalloprotein and has been previously shown to be able to catalyze polymerization of vinyl monomers under typical AGET ATRP conditions.<sup>62</sup> It was hypothesized that Hb containing iron and porphyrin can be competitive to the copper and  $\text{Me}_6\text{TREN}$  ligand used in this current research, and it was a challenge to get a balance between the catalysts in order to mediate controlled polymerization. Nevertheless, the BSA-TEG-Br and Hb-TEG-Br macroinitiators maintained water solubility and thus could be used for the aqueous SET-LRP of different hydrophilic monomers.

To demonstrate the versatility of this polymerization methodology, human lysozyme was chosen as the third protein as it has lower MW and lower water solubility when compared with BSA and Hb. Interestingly, after modification the lysozyme-TEG-Br became insoluble in water, and the white precipitate could not be dispersed well (Figure S6). The fourth peptide chosen was sCT, which is a low MW polypeptide with good water solubility. Similarly to lysozyme, the modified sCT-TEG-Br also became insoluble in water. The successful synthesis of Hb-TEG-Br, lysozyme-TEG-Br, and sCT-TEG-Br was demonstrated by MALDI-ToF MS spectroscopy (Figures S5, S7, and S9). It was hypothesized that the polymerization conditions for lysozyme-TEG-Br and sCT-TEG-Br would

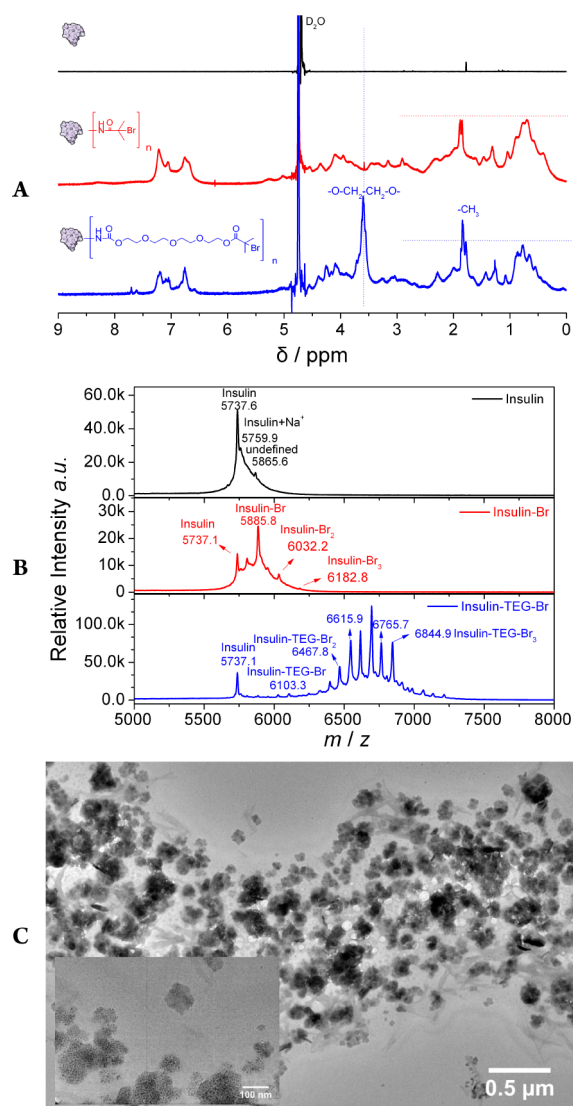
require detailed investigations due to the heterogeneity of the polymerization solutions in aqueous media.

Insulin is one of the most successfully commercialized peptide therapeutics, and yet it still encounters physical stability problems such as protein aggregation and fibril formation during production, storage, and therapy.<sup>63,64</sup> The aggregation, or fibrillation, of insulin may follow complex physical and chemical aggregation processes and is affected by a series of factors including temperature, concentration, pH, agitation, and surface properties.<sup>65,66</sup> When compared to the other four protein/peptides, insulin has poor water solubility, and  $^1\text{H}$  NMR spectroscopy even cannot reveal significant peaks for insulin in  $\text{D}_2\text{O}$  (Figure 1A).

Interestingly, after reaction the insulin-TEG-Br conjugate formed a stable colloidal suspension in water, and no precipitate was observed even after several days (Figure S13, inset). Dynamic light scattering (DLS) analysis revealed the presence of particles with average size ~160 nm (by intensity) and PDI = 0.3 (Figure S13). Further transmission electron microscopy (TEM) characterization showed that the particles had irregular shapes with varying size from ~30 to ~200 nm (Figure 1C), explaining the broad distribution observed by DLS.

In order to characterize the nanoparticles,  $^1\text{H}$  NMR, FTIR, MALDI-ToF MS and size exclusion chromatography (SEC) measurements were carried out. Subsequent to the reaction, the product dispersed well in water, and  $^1\text{H}$  NMR revealed significant peaks from tetraethylene glycol groups at ~3.6 ppm and methyl groups at ~1.9 ppm (Figure 1A). The FTIR spectrum showed strong absorbance at  $1000\text{--}1300\text{ cm}^{-1}$  due to the stretching vibration of aliphatic ether and a small ester carbonyl peak at  $\sim 1750\text{ cm}^{-1}$  (Figure S13). MALDI-ToF MS analysis showed molecular peaks from the insulin macroinitiator with mostly two or three bromine atoms per molecule (Figure 1B). Interestingly, the SEC trace of insulin-TEG-Br showed a shift when compared to native insulin due to the change in the hydrodynamic volume (Figure S13). All of these results demonstrate the successful synthesis of insulin-TEG-Br and that the products obtained form stable dispersed particles rather than soluble single peptide or an insoluble precipitate in water.

Thus, we successfully synthesized five protein and peptide macroinitiators showing different properties to enable “grafting from” polymerization in water and aqueous media, respectively. They are soluble, insoluble, or dispersible in water, making the ensuing polymerization dependent on interfacial behavior. Chemically, they contain diverse functional groups including free amines, carboxylic acids, thiols, iron, and porphyrin, etc., which may or may not affect the stability of catalyst and cause termination/side reactions in polymerization. These universal challenges exist in polymerizations from protein and peptide derived initiators, and thus any polymerization strategy developed will represent a good model for “grafting-from”



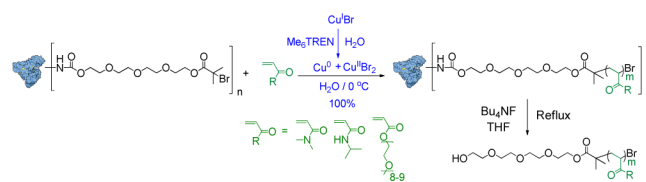
**Figure 1.** <sup>1</sup>H NMR (A) and MALDI-ToF MS spectra (B) of insulin, insulin-Br, and insulin-TEG-Br; TEM (C) of insulin-TEG-Br.

biomacromolecular initiators. It is also worth noting that the strategy utilized here lead to a mixture of macroinitiators with multiple initiation sites and will make the final conjugates a mixture as well, which theoretically did not favor the uniformity of final properties. Thus, the structure and bioactivity after conjugation were not evaluated here. Further research using maleimide-disulfide chemistry is ongoing to produce site-specific macroinitiators as well as protein–polymer conjugates with definite structures, and more results related to the activity of conjugates will be published soon.

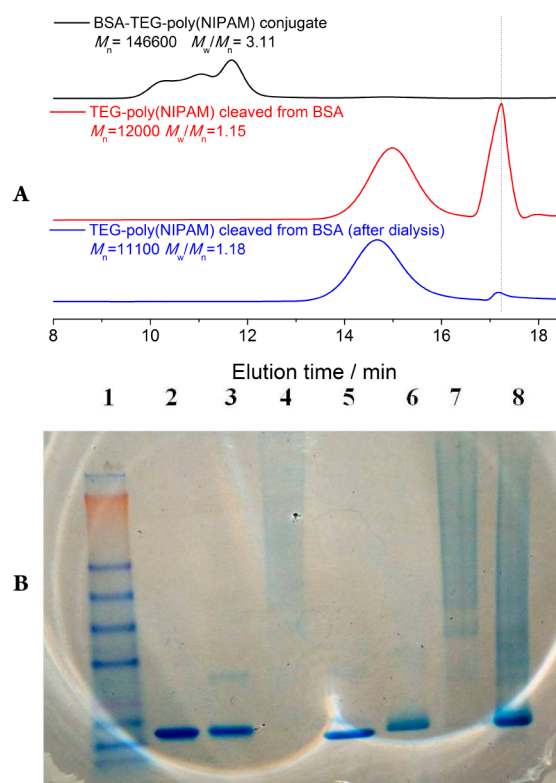
**2.2. Synthesis and Characterization of Protein/Peptide–Polymer Conjugates by Aqueous SET-LRP: Grafting from Soluble Macroinitiators.** SET-LRP is well suited for the polymerization of hydrophilic monomers in water and aqueous media. Thus, we were inspired to apply aqueous SET-LRP for the synthesis of well controlled protein/peptide–polymer conjugates (Scheme 2).

For the polymerization of NIPAM using BSA-TEG-Br as the macroinitiator, the conversion reached 86% in 30 min, and no monomer could be detected by <sup>1</sup>H NMR after 60 min (Figure S14), indicating a fast polymerization. Disappointingly, SEC chromatography of BSA-TEG-poly(NIPAM) in DMF showed a

## Scheme 2. Synthesis of BSA-polymer conjugates by aqueous SET-LRP and cleavage of polymers from BSA via carbamate deprotection



broad multiple peak ( $M_n = 146,600 \text{ g mol}^{-1}$ ,  $M_w/M_n = 3.11$ ). The shoulder peaks at 9–11 min were at first attributed to star–star coupling side reactions, occurring at high or full conversion. However, upon treatment of the conjugate with TBAF, SEC of the poly(NIPAM) cleaved from BSA exhibited a symmetrical MW distribution ( $M_n = 12,000$  and  $M_w/M_n = 1.15$ , Figure 2A), indicating that aqueous SET-LRP proceeds with



**Figure 2.** SEC elution traces of BSA-TEG-poly(NIPAM) conjugate and TEG-poly(NIPAM) (A). SDS-PAGE visualized by coomassie blue staining (B) Lane 1: protein marker, top to bottom: 250/148/98/64/50/36/22/16/6/4 kDa; Lane 2: human lysozyme; lane 3: lysozyme-TEG-Br; lane 4: lysozyme-TEG-poly(NIPAM); lane 5: bovine hemoglobin; lane 6: Hb-TEG-Br; lane 7: Hb-TEG-poly(NIPAM) by SET-LRP; and lane 8: Hb-TEG-poly(NIPAM) by enzyme-catalyzed ATRP using L-ascorbic acid as a reducing agent.

excellent control throughout the polymerization under these demanding conditions. Characterization of the cleaved polymer chains also suggests that the high MW shoulder peaks observed in the SEC of BSA-TEG-poly(NIPAM) were not the result of coupling reactions occurring during the polymerization. The BSA and BSA-TEG-Br, utilized in this work, contained several undefined protein impurities according to MALDI-ToF MS (Figure S3), and these are implicated as causes of the multiple peaks in the SEC. It is also worth noting that the tailing peak at

~17.2 min in the SEC of cleaved TEG-poly(NIPAM) was derived from small molecules (possibly salts such as TBAF etc.) and were removed via dialysis (MWCO 1000 Da) (Figure 2, A). SDS-PAGE of BSA-TEG-poly(NIPAM) showed no evidence for residual BSA macroinitiator and a band appeared at increased MW area (>250 kDa) compared with BSA-TEG-Br (Figure S4), further demonstrating the successful synthesis of BSA-TEG-poly(NIPAM) conjugate.

The polymerization of poly(ethylene glycol) methyl ether acrylate ( $M_n = 480 \text{ g mol}^{-1}$ , PEGA) and *N,N*-dimethyl acrylamide (DMA) was also performed under the same polymerization conditions with the same amount of initiator, solvent, and catalyst. The polymerizations of PEGA and DMA were also fast with conversion reaching 94% and 91%, respectively, after 90 min (Figures S21 and S24). Following cleavage of the polymers from the conjugates, SEC analysis of the TEG-poly(PEGA) and TEG-poly(DMA) presented a final  $M_n = 19,800 \text{ g mol}^{-1}$ ,  $M_w/M_n = 1.29$  and  $M_n = 12,900 \text{ g mol}^{-1}$ ,  $M_w/M_n = 1.30$ , respectively (Figure S27).

Although the cleaved polymers had good MW distributions, the catalyst ratio was optimized in order to improve the control. The amount of CuBr was doubled while maintaining the same level of  $\text{Me}_6\text{TREN}$ , in which case the disproportionation still went to completion and additional  $\text{CuBr}_2$  as deactivator was introduced to the system. The polymerization of PEGA under these conditions gave 80% conversion after 90 min and 91% after 4 h. The polymerization yielded TEG-poly(PEGA) with  $M_n = 22,700 \text{ g mol}^{-1}$ ,  $M_w/M_n = 1.21$  (Figure S27), indicating improved control. Likewise, for the polymerization of DMA, the increased CuBr also improved the control ( $M_n = 13,200 \text{ g mol}^{-1}$ ,  $M_w/M_n = 1.22$ , Figure S27).

AGET ATRP of NIPAM from BSA-TEG-Br using  $\text{Me}_6\text{TREN}$  as the ligand was also performed as a control experiment, which showed a lower polymerization rate than SET-LRP with 70% conversion after 100 min and close to full conversion after leaving for 20 h (Figure S19). The final cleaved TEG-poly(NIPAM) from BSA still showed relatively narrow MW distribution ( $M_w/M_n = 1.17$ ) under the same SEC test conditions. It is noted that the  $\text{Me}_6\text{TREN}$  ligand has not generally been used for aqueous AGET ATRP as it is approximately 15 times more reactive than TPMA, which would make the activation rate even higher and thus polymerization more difficult to control.<sup>67</sup> In addition we utilized an excess of *L*-ascorbic acid ( $[\text{CuBr}_2]: [\text{L-ascorbic acid}] = 2:1$ ) rather than 1% of *L*-ascorbic relative to  $\text{CuBr}_2$ . This was directly added to the system in a one shot rather than by slow addition over 4 h as previously reported.<sup>17</sup>

In summary, well-defined BSA-polymer conjugates were synthesized by aqueous SET-LRP with an excess of CuBr relative to  $\text{Me}_6\text{TREN}$  favoring better control during polymerization leading to final polymers with narrow MW distribution less than or close to 1.20.

Subsequently, we investigated the synthesis of Hb-polymer conjugates. Interestingly, Hb contains heme centers, which have been reported to have some ability to mediate polymerization of hydrophilic monomers using an organic initiator under apparent AGET ATRP conditions.<sup>62,68</sup> The Hb-TEG-Br macroinitiator contains both a heme center and an organobromine initiating site itself, and this inspired us to attempt polymerization using Hb-TEG-Br as both the initiator and the catalyst precursor. Hb-TEG-Br and NIPAM monomer were added to a deoxygenated solution in water, and then *L*-ascorbic acid was added prior to leaving for 21 h. <sup>1</sup>H NMR

revealed that the conversion only reached 38% (Figure S28). SDS-PAGE revealed a significant initiator residue at ~16 kD and a broad band from ~20 kD to >250 kD, suggesting the *in situ* polymerization and protein-polymer conjugation did occur but was not efficient (Figure 2B). SEC of the cleaved TEG-poly(NIPAM) revealed a broad peak ( $M_w/M_n = 2.74$ ) with tailing at the low MW position, suggesting possible termination during the early stages of polymerization (Figure S29). Unlike polymerization from the small molecule initiator, it is hypothesized that the heme centers located within Hb could not access the macroinitiator site. Thus, the initiation was not efficient, and polymerization tends to be uncontrolled due to inefficient deactivation.

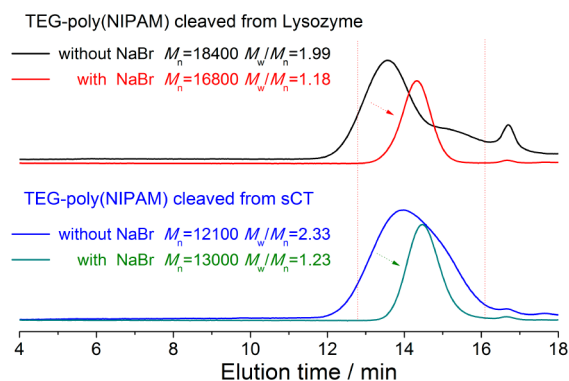
This led to work focusing on polymerization grafting from Hb in the presence of a copper catalyst. However, it should be noted that  $\text{Cu}^{\text{II}}$  is able to bind/oxidize Hb.<sup>69,70</sup> Thus, there should be less free  $\text{Cu}^{\text{II}}$  available as the deactivator for SET-LRP due to possible interactions and/or exchange with the heme centers. Furthermore, the iron porphyrin from the heme may still act as an additional catalyst adding further complexity to the system. In a test polymerization of NIPAM using  $[\text{CuBr}]:[\text{Me}_6\text{TREN}] = 1:1$ , monomer conversion reached 34% after 6 h, suggesting that the catalyst ratio was not ideal. Increasing the amount of  $\text{Me}_6\text{TREN}$  ( $[\text{CuBr}]:[\text{Me}_6\text{TREN}] = 1:2$ ), for the polymerization of both NIPAM and PEGA resulted in full conversion after 1.5 and 4.5 h, respectively. SEC analysis of the cleaved polymers revealed relatively broad MW distributions with  $M_n = 17,800 \text{ g mol}^{-1}$ ,  $M_w/M_n = 2.80$  for TEG-poly(NIPAM) and  $M_n = 8,600 \text{ g mol}^{-1}$ ,  $M_w/M_n = 1.62$  for TEG-poly(PEGA) (Figures S30 and S31). SDS-PAGE did not reveal significant macroinitiator residues, suggesting the initiation by SET-LRP was efficient compared with the *in situ* AGET ATRP (Figure 2B). When the ratio of  $[\text{CuBr}]:[\text{Me}_6\text{TREN}]$  was decreased to 1:1.5, the polymerization of NIPAM became slower as the conversion only reached 62% in 1.5 h and 88% in 4.5 h. However, the final polymer had a narrower MW distribution, and the  $M_w/M_n$  decreased from 2.80 to 1.68 (Figure S30). It needs to be noted that nitrogen bubbling cannot effectively remove oxygen from hemoglobin like carbon monoxide and the free cysteine groups in hemoglobin were also not blocked, which may affect the grafting efficiency or increase the possibility of termination or chain transfer reactions during polymerization.

Thus, grafting from Hb was inefficient via *in situ* catalyzed AGET ATRP, while SET-LRP could mediate fast polymerizations from Hb, although the final polymers generally had broad MW distributions ( $M_w/M_n > 1.6$ ), which is ascribed to interference from Hb.

**2.3. Grafting from Insoluble Macroinitiators via Aqueous SET-LRP: Effect of Protein Denaturant and NaBr.** Direct use of the insoluble macroinitiator lysozyme-TEG-Br for aqueous SET-LRP showed no significant polymerization according to <sup>1</sup>H NMR (Figure S33). It was hypothesized that the  $\text{Cu}^0$  activators could not interact with the initiation sites on the insoluble protein precipitate. In an attempt to solve this problem we attempted to solubilize the macroinitiator such that the organobromine could react with the surface  $\text{Cu}^0$  atoms on the  $\text{Cu}^0$  powders. Protein solubility is a common problem encountered and various denaturants such as urea, guanidine, 2-mercaptoethanol, and sodium dodecyl sulfate (SDS) etc. have been used to break the interactions involved in protein aggregation and aid dissolution. Among these denaturants, SDS acts by coating the protein with

uniform negative charge, which can disrupt the chain folding of native protein, leaving the primary structure unaffected.

Thus, protein macroinitiators were first solubilized in 0.5% SDS with different monomers prior to addition of catalyst.  $^1\text{H}$  NMR used to monitor the reaction revealed fast polymerizations of NIPAM and PEGA from lysozyme or sCT. Full conversions were obtained in <90 min (Figure S34). SDS-PAGE confirmed the successful synthesis of a lysozyme-TEG-poly(NIPAM) conjugate with disappearance of macroinitiator (Figure 2B). However, SEC analysis of cleaved polymers showed a relatively broad MW distribution ( $M_w/M_n \geq \sim 2$ , Figure 3). The poor control was attributed to the loss of halide



**Figure 3.** SEC elution traces of TEG-poly(NIPAM) cleaved from lysozyme and sCT for the SET-LRP in 0.5% SDS solution with or without excess NaBr.

anions mediated by SDS, which has also been considered as a general phenomenon in the ATRP emulsion polymerization with an anionic surfactant.<sup>71,72</sup> As a control experiment, we carried out the polymerization of NIPAM grafting from BSA in 0.5% SDS solution instead of water. The final polymer exhibited a much broader MW distribution with  $M_w/M_n$  increased from 1.18 to 1.46 (Figure S18), confirming that SDS has a detrimental effect on the polymerization.

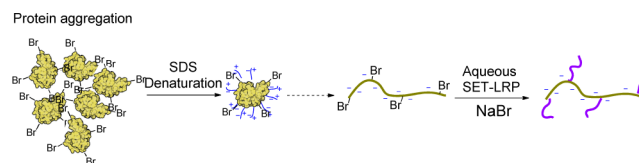
In one recent report an excess of halide salts was shown to be able to minimize deactivator loss when SDS was used as the surfactant in ATRP under miniemulsion conditions.<sup>72</sup> A similar strategy was thus utilized by adding excess NaBr to the SDS solution.  $^1\text{H}$  NMR did not reveal significant differences in the polymerization rate yet the polymers cleaved from lysozyme or sCT obviously had much narrower MW distribution ( $M_w/M_n = 1.18$  or  $1.23$ , Figure 3), suggesting the effectiveness of NaBr in aiding better control.

Interestingly, we noticed that sufficient L-ascorbic acid could help the sCT macroinitiator to be solubilized in water. Thus, AGET ATRP of NIPAM from sCT-TEG-Br (10 mg,  $2.4 \mu\text{mol}$ ) was performed using excess L-ascorbic acid (10 mg,  $57 \mu\text{mol}$ ). In these polymerizations, high conversion ( $\sim 80\%$ ) could be obtained after reaction for 19 h, and the final polymer had relatively high  $M_w/M_n$  value ranging from 1.6–1.9 (Figure S38), possibly due to there being insufficient  $\text{CuBr}_2$  for efficient deactivation considering excess reducing agent was utilized in these reactions.

In summary, protein denaturation was required in order to solubilize lysozyme and sCT macroinitiators in water for effective SET-LRP. The presence of SDS resulted in poor control over MW distribution yet addition of an excess NaBr resulted in much improved control. The L-ascorbic acid also helped protein solubilization, and a sCT-polymer conjugate

could be synthesized via AGET ATRP without the use of SDS and NaBr. These strategies could favor polymer conjugation from insoluble protein/peptides, and different kinds of denaturants especially cationic and nonionic type detergents may be more compatible with this SET-LRP system (Scheme 3).

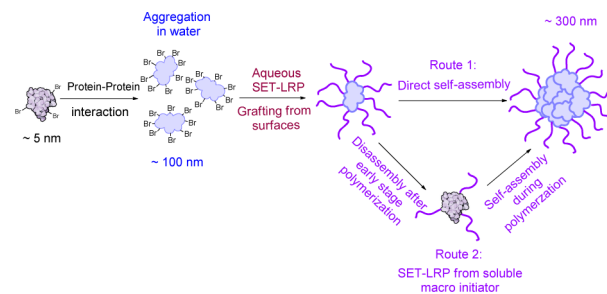
### Scheme 3. Synthesis of Lysozyme–Polymer Conjugates by Aqueous SET-LRP in the Presence of SDS and NaBr



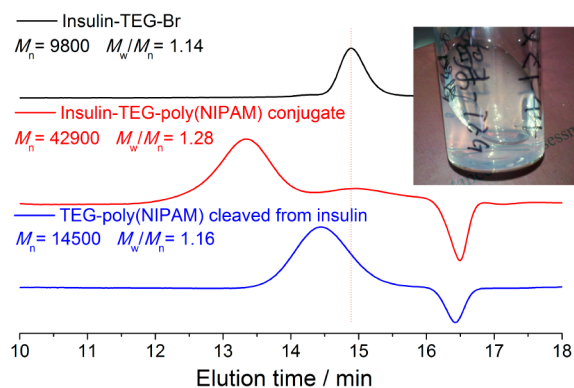
### 2.4. Grafting from Dispersed Protein Particles by Aqueous SET-LRP: Surface Chemistry, Self-Assembly and Disassembly.

Although low pH will favor solubilization of insulin in water, it would protonate the amine ligand and catalyst complex, which also makes it a challenge to polymerize acidic monomers using this system. Thus, it tends to be not available to polymerize from solubilized insulin macroinitiator at low pH. However, theoretically SET-LRP would also work in heterogeneous system, and it is possible to directly graft polymers from the surface as long as the initiator has chance to interact with the copper catalyst.  $\text{Cu}^0$  wire-mediated SET-LRP has been successfully applied for the surface functionalization of polymer latex in water to form core–shell type particles with functional polymer brushes.<sup>73</sup> The insulin-TEG-Br formed a stable colloidal suspension in water, and the charged insulin supplied stability for the protein aggregates in a similar way as SDS for a latex particle, which made it suitable for SET-LRP in water. Thus, the first step in this reaction should be polymerization grafting from the surface of protein aggregates (Scheme 4).

### Scheme 4. Schematic Representation for the Preparation of Insulin-TEG-Polymer Conjugates and Possible Self-Assembly Mechanism



For the polymerization of NIPAM from insulin,  $^1\text{H}$  NMR revealed fast polymerization reaching 75% conversion in 60 min and 100% after leaving for 19 h (Figure S39). Interestingly, the SEC of the insulin-TEG-poly(NIPAM) conjugate showed a relatively narrow peak with clear tailing to low MW (Figure 4), which coincided with the macroinitiator peak. It is hypothesized that the macroinitiators that are wrapped inside the protein particles have less chance to interact with the copper catalyst and/or monomer limiting initiation and propagation within the particle core. The TEG-poly(NIPAM) cleaved from insulin showed a narrow MW distribution with  $M_n = 14,500$

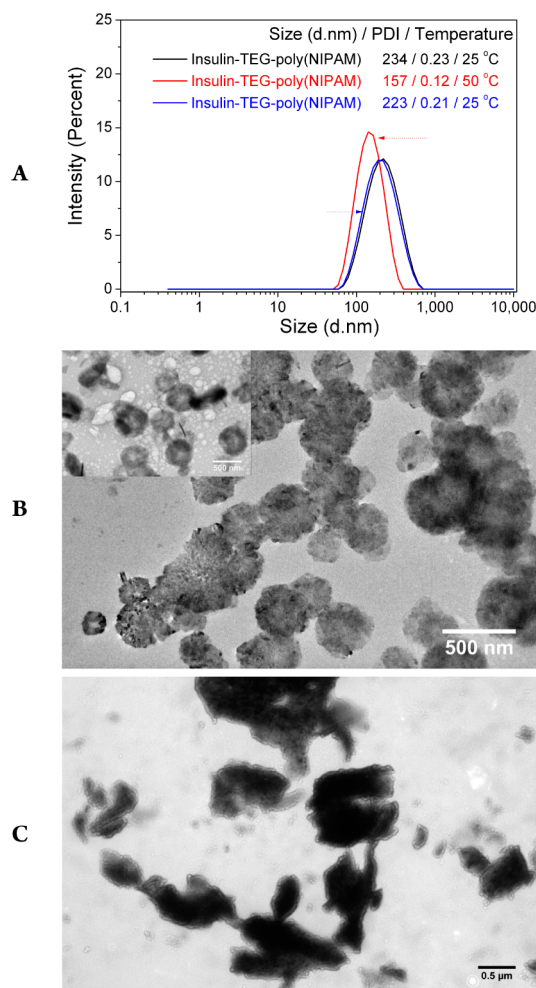


**Figure 4.** SEC elution traces of insulin-TEG-Br, insulin-TEG-poly(NIPAM), and TEG-poly(NIPAM) after deprotection (the inset is stable colloidal suspension of insulin-TEG-poly(NIPAM) in water).

and  $M_w/M_n = 1.16$  (Figure 4), indicating excellent control over MW and MW distribution when grafting from the protein particle surface. The  $^1\text{H}$  NMR spectra of the insulin-TEG-poly(NIPAM) conjugate and TEG-poly(NIPAM) revealed all typical peaks from poly(NIPAM) (Figure S41). The MALDI-ToF MS spectrum (Figure S42) of TEG-poly(NIPAM) showed a series of peaks with typical NIPAM MW peak intervals, which support the formation of an insulin-TEG-poly(NIPAM) conjugate. Furthermore, cloud point tests by UV-vis spectroscopy demonstrated different behaviors at elevated temperature. For the clear TEG-poly(NIPAM) solution, the aggregation had a narrow temperature window for the cloud point temperature ranging from  $\sim 47$  to  $\sim 50$  °C. Despite the insulin-TEG-poly(NIPAM) conjugates existing as a colloidal suspension in water (Figure 4, inset), aggregation started from  $\sim 40$  to  $>60$  °C (Figure S43).

All of these characterizations strongly suggested the successful synthesis of insulin-TEG-poly(NIPAM) conjugates. Subsequent TEM characterization of insulin-TEG-poly(NIPAM) suspensions showed the existence of regularly shaped spheres with a diameter ranging from 200 to 400 nm (Figure 5B). This led us to think about the formation mechanism of such microspheres. First, we believed these spheres were formed via self-assembly of protein particles (core)-poly(NIPAM) brush (shell) during the polymerization (Scheme 4, Route 1). However, most of these spheres had a regular shape and similar sizes as opposed to random structures of insulin macroinitiator with varied size. It is also possible that at the early stage of the polymerization the hydrophobic sites changed into hydrophilic chains, which may lead to disassembly of the protein aggregates to form soluble protein macroinitiators. These initiators are able to continue the polymerization in solution which may induce further self-assembly, forming microspheres with relative defined shape and size (Scheme 4, Route 2).

Subsequently, different monomers including PEGA and a mannose functional glycomonomer (ManA), synthesized via Fischer glycosylation and azide-alkyne click reaction,<sup>24,74</sup> were further tested for polymerization from insulin. The polymerization of acrylate monomers generally showed poor control over MW distribution as compared to acrylamides (Figures S44 and S46). The living nature and chain-end fidelity of the polymerization chain extension to form insulin-TEG-poly(NIPAM)-*b*-(ManA) was successfully performed via a one-pot strategy (Figures S47–S50). Besides, the control polymer-



**Figure 5.** DLS of insulin-TEG-poly(NIPAM) at different temperature (A). TEM images of insulin-TEG-poly(NIPAM) (B) and insulin-TEG-poly(ManA) (B, inset). Aggregation of insulin-TEG-poly(ManA) after addition of ConA (C).

izations from insulin with noncleavable amide-derived initiators were also successfully conducted (Figures S51–S54), which all showed fast polymerization rate and high chain end fidelity for block copolymerization.

In summary, various insulin-polymer conjugates were synthesized via aqueous SET-LRP from the surface of protein particles. The self-assembly of conjugates in water formed nano to micro spheres through either direct self-assembly or first disassembly following further self-assembly during polymerization, which needs further research to confirm.

**2.5. Controlled Self-Assembly of Protein-Polymer Conjugates: Thermal Control, Carbohydrate-Protein Interaction, and SDS Denaturation.** Polymerization grafting from insulin resulted in a white suspension with an appearance similar to polymer latexes (Figure 4, inset). Even after dialysis and lyophilization the obtained solid product still formed a stable suspension when redispersed in water. Both DLS and TEM were used to evaluate the structure and property of these suspensions. DLS of insulin-TEG-poly(NIPAM) revealed the presence of particles with average intensity size of 234 nm with PDI = 0.23 (Figure 5A), indicating a larger size yet decreased PDI than insulin-TEG-Br, which demonstrated the successful synthesis and also suggested that the self-assembly may lead to a more uniform morphology rather than random aggregates.

TEM characterization confirmed spheres with a regular round shape (Figure 5B), although the spheres had different sizes ranging from ~100 to ~400 nm.

When the temperature of the suspension was increased from 25 to 50 °C, DLS revealed a decrease both in size and PDI, suggesting the sphere may have collapsed due to the LCST behavior of poly(NIPAM), which simultaneously decreased the size difference between each sphere and led to smaller PDI. When the temperature was decreased to 25 °C, the size increased to 223 nm with PDI to 0.21, indicating a reversible thermally controlled size change. Similarly, DLS and TEM analysis confirmed the existence of spheres for insulin-TEG-poly(ManA) (Figure 5B inset and Figure S56), which can be considered as a kind of glycoprotein particles. In order to confirm the presence of functional glycopolymer chains on the surface, we added an excess of concanavalin A (ConA) to the glycoprotein suspension for DLS and TEM monitoring. ConA is a lectin and binds specifically to glycoproteins and glycolipids containing mannose and glucose moieties, which has been widely used in glycoparticle research.<sup>75,76</sup>

Due to the carbohydrate–protein interactions the surface glycopolymer from different particles should be able to recognize ConA and cause particle aggregation, as the ConA has a tetramer structure and multiple binding sites for mannose. As expected, the DLS revealed a significant size and PDI increase after addition of ConA over several minutes and a precipitate with particle size >1000 nm detected (Figure S56).

TEM analysis demonstrated the disappearance of spheres yet showed the presence of bulk solid with particle sizes up to several micrometres (Figure 5C), which could be caused by the aggregation of glycoparticles. As a control experiment, ConA was also added to the insulin-TEG-poly(NIPAM) suspensions, however, DLS revealed no significant change over size or PDI (Figure S55), indicating no significant interactions between ConA and insulin or poly(NIPAM).

We believe the formation of these spheres derives from the self-assembly of insulin–polymer conjugates, mainly driven by the hydrophobicity of insulin. Thus, changing the solubility of insulin might change or even destroy the self-assembled structure (Scheme 5). In order to verify this assumption, SDS was added to a suspension of insulin-TEG-poly(ManA) and left for 1 h.

Subsequently, DLS revealed a sharp peak with different size and a broad PDI suggesting the results were not reliable

(Figure S56), indicating possible changes to native sphere. TEM confirmed the disappearance of spheres, and the dark area presented polymers coated densely on the copper grid (Figure S56), which proved the total destruction of the spheres and also explained the poor results from DLS. Thus, the denaturation changed the chain folding of insulin, increased its water-solubility, and further caused disassembly of the insulin–polymer conjugate spheres.

In summary, the insulin–polymer conjugates formed spherical structures in water. Depending on the properties of surface polymer brushes, the self-assembly could be controlled utilizing either thermal control or carbohydrate–protein interaction.

### 3. CONCLUSION

In conclusion, Cu-LRP, more specifically SET-LRP, has been introduced for successful synthesis of well-defined protein/peptide–polymer conjugates with full characterization. The SET-LRP system utilized a prior disproportionation strategy to generate the active copper catalyst, which could be easily handled in the lab. Polymerizations were performed in water without the use of any organic solvents and generally at ambient temperature or below (0 °C) in order to obtain better control, representing very mild and biologically benign conditions for the fragile biomacromolecules. Fast and full monomer conversion could be generally obtained in minutes to several hours. Copper catalysts were easily removed via filtration following dialysis against water. The lyophilized products were colorless, and other compounds purified following the same procedure showed no observable cytotoxicity effect to green monkey kidney cells in our ongoing test.

A library of protein/peptides with different physical and chemical properties were modified as macroinitiators and optimized polymerization conditions ensured successful polymerization from soluble, insoluble, and dispersed protein/peptide single molecules or aggregates. Different kinds of acrylamide and acrylate monomers were compatible with this system for homo and block copolymerization to generate hydrophilic polymers with controlled MW and narrow MW distribution. Polymerizations from insulin macroinitiators followed “grafting from” surface-initiated polymerization conditions and may be involved in complex and interesting self-assembly and disassembly processes. These insulin–polymer conjugates formed spheres in water, and the assembly behavior could be controlled via thermal, carbohydrate–protein interaction and SDS denaturation.

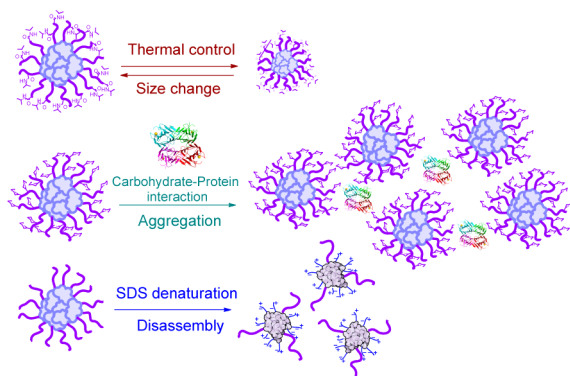
The polymerization strategy utilized in this research is facile, versatile, relatively inexpensive, and biologically benign. We believe our design supplies useful information and suggestions for polymer conjugation from different protein/peptides, and it will promote the research and development in protein therapeutic and drug delivery.

### ■ ASSOCIATED CONTENT

#### Supporting Information

Experimental details and supplementary data including NMR, SEC, UV–vis, FTIR, and MALDI-ToF MS. The Supporting Information is available free of charge on the ACS Publications website at DOI: 10.1021/jacs.5b04139.

**Scheme 5. Schematic Representation for the Controlled Self-Assembly of Insulin–Polymer Conjugates via Thermal Control, Carbohydrate–Protein Interaction and SDS Denaturation**





## ■ AUTHOR INFORMATION

## Corresponding Author

\*D.M.Haddleton@warwick.ac.uk

## Notes

The authors declare no competing financial interest.

## ■ ACKNOWLEDGMENTS

Q.Z. acknowledges the financial support from University of Warwick and China Scholarship Council. Some of the equipment used was supported by the Innovative Uses for Advanced Materials in the Modern World (AM2), with support from Advantage West Midlands (AWM) and partially funded by the European Regional Development Fund (ERDF). D.M.H. is a Royal Society/Wolfson Fellow. Protein structures used in this research are from RCSB Protein Data Bank and produced by Dr. David S. Goodsell.

## ■ REFERENCES

- (1) Katre, N. V. *Adv. Drug Delivery Rev.* **1993**, *10*, 91.
- (2) Caliceti, P.; Veronese, F. M. *Adv. Drug Delivery Rev.* **2003**, *55*, 1261.
- (3) Pelegri-O'Day, E. M.; Lin, E.-W.; Maynard, H. D. *J. Am. Chem. Soc.* **2014**, *136*, 14323.
- (4) Wang, Y.-S.; Youngster, S.; Grace, M.; Bausch, J.; Bordens, R.; Wyss, D. F. *Adv. Drug Delivery Rev.* **2002**, *54*, 547.
- (5) Alconcel, S. N. S.; Baas, A. S.; Maynard, H. D. *Polym. Chem.* **2011**, *2*, 1442.
- (6) Yamaoka, T.; Tabata, Y.; Ikada, Y. *J. Pharm. Sci.* **1994**, *83*, 601.
- (7) Knop, K.; Hoogenboom, R.; Fischer, D.; Schubert, U. S. *Angew. Chem., Int. Ed.* **2010**, *49*, 6288.
- (8) Broyer, R. M.; Grover, G. N.; Maynard, H. D. *Chem. Commun.* **2011**, *47*, 2212.
- (9) Wang, J.-S.; Matyjaszewski, K. *J. Am. Chem. Soc.* **1995**, *117*, 5614.
- (10) Bontempo, D.; Maynard, H. D. *J. Am. Chem. Soc.* **2005**, *127*, 6508.
- (11) Heredia, K. L.; Bontempo, D.; Ly, T.; Byers, J. T.; Halstenberg, S.; Maynard, H. D. *J. Am. Chem. Soc.* **2005**, *127*, 16955.
- (12) Lele, B. S.; Murata, H.; Matyjaszewski, K.; Russell, A. J. *Biomacromolecules* **2005**, *6*, 3380.
- (13) Nicolas, J.; Miguel, V. S.; Mantovani, G.; Haddleton, D. M. *Chem. Commun.* **2006**, 4697.
- (14) Tsarevsky, N. V.; Matyjaszewski, K. *Chem. Rev.* **2007**, *107*, 2270.
- (15) He, W.; Jiang, H.; Zhang, L.; Cheng, Z.; Zhu, X. *Polym. Chem.* **2013**, *4*, 2919.
- (16) Tsarevsky, N. V.; Braunecker, W. A.; Matyjaszewski, K. *J. Organomet. Chem.* **2007**, *692*, 3212.
- (17) Averick, S.; Simakova, A.; Park, S.; Konkolewicz, D.; Magenau, A. J. D.; Mehl, R. A.; Matyjaszewski, K. *ACS Macro Lett.* **2012**, *1*, 6.
- (18) Magnusson, J. P.; Bersani, S.; Salmaso, S.; Alexander, C.; Caliceti, P. *Bioconjugate Chem.* **2010**, *21*, 671.
- (19) Zhu, B.; Lu, D.; Ge, J.; Liu, Z. *Acta Biomater.* **2011**, *7*, 2131.
- (20) Percec, V.; Popov, A. V.; Ramirez-Castillo, E.; Monteiro, M.; Barboiu, B.; Weichold, O.; Asandei, A. D.; Mitchell, C. M. *J. Am. Chem. Soc.* **2002**, *124*, 4940.
- (21) Percec, V.; Guliasvili, T.; Ladislav, J. S.; Wistrand, A.; Stjern Dahl, A.; Sienkowska, M. J.; Monteiro, M. J.; Sahoo, S. *J. Am. Chem. Soc.* **2006**, *128*, 14156.
- (22) Rosen, B. M.; Percec, V. *Chem. Rev.* **2009**, *109*, 5069.
- (23) Soeriyadi, A. H.; Boyer, C.; Nyström, F.; Zetterlund, P. B.; Whittaker, M. R. *J. Am. Chem. Soc.* **2011**, *133*, 11128.
- (24) Zhang, Q.; Collins, J.; Anastasaki, A.; Wallis, R.; Mitchell, D. A.; Becer, C. R.; Haddleton, D. M. *Angew. Chem., Int. Ed.* **2013**, *52*, 4435.
- (25) Zhang, Q.; Su, L.; Collins, J.; Chen, G.; Wallis, R.; Mitchell, D. A.; Haddleton, D. M.; Becer, C. R. *J. Am. Chem. Soc.* **2014**, *136*, 4325.
- (26) Samanta, S. R.; Cai, R.; Percec, V. *Polym. Chem.* **2014**, *5*, 5479.
- (27) Levere, M. E.; Nguyen, N. H.; Leng, X.; Percec, V. *Polym. Chem.* **2013**, *4*, 1635.
- (28) Levere, M. E.; Nguyen, N. H.; Sun, H.-J.; Percec, V. *Polym. Chem.* **2013**, *4*, 686.
- (29) Nguyen, N. H.; Rosen, B. M.; Jiang, X.; Fleischmann, S.; Percec, V. J.; *Polym. Sci., A. J. Polym. Sci., Part A: Polym. Chem.* **2009**, *47*, 5577.
- (30) Lligadas, G.; Percec, V. J.; *Polym. Sci., A. J. Polym. Sci., Part A: Polym. Chem.* **2008**, *46*, 6880.
- (31) Zhang, Q.; Wilson, P.; Li, Z.; McHale, R.; Godfrey, J.; Anastasaki, A.; Waldron, C.; Haddleton, D. M. *J. Am. Chem. Soc.* **2013**, *135*, 7355.
- (32) Nguyen, N. H.; Kulis, J.; Sun, H.-J.; Jia, Z.; van Beusekom, B.; Levere, M. E.; Wilson, D. A.; Monteiro, M. J.; Percec, V. *Polym. Chem.* **2013**, *4*, 144.
- (33) McKenzie, T. G.; Wong, E. H. H.; Fu, Q.; Lam, S. J.; Dunstan, D. E.; Qiao, G. G. *Macromolecules* **2014**, *47*, 7869.
- (34) Xue, L.; Lyu, Z.; Shi, X.; Tang, Z.; Chen, G.; Chen, H. *Macromol. Chem. Phys.* **2014**, *215*, 1491.
- (35) Keskin, D.; Clodt, J. I.; Hahn, J.; Abetz, V.; Filiz, V. *Langmuir* **2014**, *30*, 8907.
- (36) Anastasaki, A.; Haddleton, A. J.; Zhang, Q.; Simula, A.; Droesbeke, M.; Wilson, P.; Haddleton, D. M. *Macromol. Rapid Commun.* **2014**, *35*, 965.
- (37) Boyer, C.; Zetterlund, P. B.; Whittaker, M. R. J.; *Polym. Sci., A. J. Polym. Sci., Part A: Polym. Chem.* **2014**, *52*, 2083.
- (38) Nguyen, N. H.; Rodriguez-Emmenegger, C.; Brynda, E.; Sedlakova, Z.; Percec, V. *Polym. Chem.* **2013**, *4*, 2424.
- (39) Zhang, Q.; Li, Z.; Wilson, P.; Haddleton, D. M. *Chem. Commun.* **2013**, *49*, 6608.
- (40) Zhang, Q.; Wilson, P.; Anastasaki, A.; McHale, R.; Haddleton, D. M. *ACS Macro Lett.* **2014**, *3*, 491.
- (41) Waldron, C.; Zhang, Q.; Li, Z.; Nikolaou, V.; Nurumbetov, G.; Godfrey, J.; McHale, R.; Yilmaz, G.; Randev, R. K.; Girault, M.; McEwan, K.; Haddleton, D. M.; Droesbeke, M.; Haddleton, A. J.; Wilson, P.; Simula, A.; Collins, J.; Lloyd, D. J.; Burns, J. A.; Summers, C.; Houben, C.; Anastasaki, A.; Li, M.; Becer, C. R.; Kiviahio, J. K.; Risangud, N. *Polym. Chem.* **2014**, *5*, 57.
- (42) Moad, G.; Rizzardo, E.; Thang, S. H. *Aust. J. Chem.* **2005**, *58*, 379.
- (43) Boyer, C.; Bulmus, V.; Davis, T. P.; Ladmiral, V.; Liu, J.; Perrier, S. *Chem. Rev.* **2009**, *109*, 5402.
- (44) Moad, G.; Rizzardo, E.; Thang, S. H. *Aust. J. Chem.* **2012**, *65*, 985.
- (45) De, P.; Li, M.; Gondi, S. R.; Sumerlin, B. S. *J. Am. Chem. Soc.* **2008**, *130*, 11288.
- (46) Li, X.; Wang, L.; Chen, G.; Haddleton, D. M.; Chen, H. *Chem. Commun.* **2014**, *50*, 6506.
- (47) Xu, J.; Jung, K.; Corrigan, N. A.; Boyer, C. *Chem. Sci.* **2014**, *5*, 3568.
- (48) Liu, J.; Bulmus, V.; Herlambang, D. L.; Barner-Kowollik, C.; Stenzel, M. H.; Davis, T. P. *Angew. Chem., Int. Ed.* **2007**, *46*, 3099.
- (49) Boyer, C.; Bulmus, V.; Liu, J.; Davis, T. P.; Stenzel, M. H.; Barner-Kowollik, C. *J. Am. Chem. Soc.* **2007**, *129*, 7145.
- (50) Barbucci, R.; Casolaro, M.; Magnani, A. *Polym. J.* **1989**, *21*, 915.
- (51) Teodorescu, M.; Matyjaszewski, K. *Macromolecules* **1999**, *32*, 4826.
- (52) Chapman, R.; Jolliffe, K. A.; Perrier, S. *Polym. Chem.* **2011**, *2*, 1956.
- (53) Danial, M.; Tran, C. M. N.; Jolliffe, K. A.; Perrier, S. *J. Am. Chem. Soc.* **2014**, *136*, 8018.
- (54) ten Cate, M. G. J.; Severin, N.; Börner, H. G. *Macromolecules* **2006**, *39*, 7831.
- (55) Top, A.; Zhong, S.; Yan, C.; Roberts, C. J.; Pochan, D. J.; Kiick, K. L. *Soft Matter* **2011**, *7*, 9758.
- (56) Huang, X.; Li, M.; Green, D. C.; Williams, D. S.; Patil, A. J.; Mann, S. *Nat. Commun.* **2013**, *4*, 2239.
- (57) Lam, C. N.; Kim, M.; Thomas, C. S.; Chang, D.; Sanoja, G. E.; Okwara, C. U.; Olsen, B. D. *Biomacromolecules* **2014**, *15*, 1248.
- (58) Chang, D.; Lam, C. N.; Tang, S.; Olsen, B. D. *Polym. Chem.* **2014**, *5*, 4884.

- (59) Cummings, C.; Murata, H.; Koepsel, R.; Russell, A. J. *Biomaterials* **2013**, *34*, 7437.
- (60) Cummings, C.; Murata, H.; Koepsel, R.; Russell, A. J. *Biomacromolecules* **2014**, *15*, 763.
- (61) Jacquemard, U.; Bénêteau, V.; Lefoix, M.; Routier, S.; Mérour, J.-Y.; Coudert, G. *Tetrahedron* **2004**, *60*, 10039.
- (62) Silva, T. B.; Spulber, M.; Kocik, M. K.; Seidi, F.; Charan, H.; Rother, M.; Sigg, S. J.; Renggli, K.; Kali, G.; Bruns, N. *Biomacromolecules* **2013**, *14*, 2703.
- (63) Wang, W. *Int. J. Pharm.* **2005**, *289*, 1.
- (64) Nielsen, L.; Khurana, R.; Coats, A.; Frokjaer, S.; Brange, J.; Vyas, S.; Uversky, V. N.; Fink, A. L. *Biochemistry* **2001**, *40*, 6036.
- (65) Sluzky, V.; Tamada, J. A.; Klibanov, A. M.; Langer, R. *Proc. Natl. Acad. Sci. U. S. A.* **1991**, *88*, 9377.
- (66) Dzwolak, W.; Ravindra, R.; Lendermann, J.; Winter, R. *Biochemistry* **2003**, *42*, 11347.
- (67) Tang, W.; Kwak, Y.; Braunecker, W.; Tsarevsky, N. V.; Coote, M. L.; Matyjaszewski, K. *J. Am. Chem. Soc.* **2008**, *130*, 10702.
- (68) Simakova, A.; Mackenzie, M.; Averick, S. E.; Park, S.; Matyjaszewski, K. *Angew. Chem., Int. Ed.* **2013**, *52*, 12148.
- (69) Manoharan, P. T.; Alston, K.; Rifkind, J. M. *Biochemistry* **1989**, *28*, 7148.
- (70) Rifkind, J. M.; Lauer, L. D.; Chiang, S. C.; Li, N. C. *Biochemistry* **1976**, *15*, 5337.
- (71) Matyjaszewski, K.; Qiu, J.; Shipp, D. A.; Gaynor, S. G. *Macromol. Symp.* **2000**, *155*, 15.
- (72) Teo, V. L.; Davis, B. J.; Tsarevsky, N. V.; Zetterlund, P. B. *Macromolecules* **2014**, *47*, 6230.
- (73) Chabrol, V.; Léonard, D.; Zorn, M.; Reck, B.; D'Agosto, F.; Charleux, B. *Macromolecules* **2012**, *45*, 2972.
- (74) Zhang, Q.; Slavin, S.; Jones, M. W.; Haddleton, A. J.; Haddleton, D. M. *Polym. Chem.* **2012**, *3*, 1016.
- (75) Chen, G.; Tao, L.; Mantovani, G.; Geng, J.; Nyström, D.; Haddleton, D. M. *Macromolecules* **2007**, *40*, 7513.
- (76) Ting, S. R. S.; Min, E. H.; Zetterlund, P. B.; Stenzel, M. H. *Macromolecules* **2010**, *43*, 5211.